Towards IMU/UWB Fusion based Localization: Error Modeling and Spatial-Temporal Performance Evaluation

Cheng Xu[1,2], Jie He[1,2], Xiaotong Zhang[1,2]
[1]School of Computer and Communication Engineering, University of Science and Technology Beijing
[2]Beijing Key Laboratory of Knowledge Engineering for Materials Science
Email: xucheng@ieee.org, hejie@ustb.edu.cn, zxt@ies.ustb.edu.cn

***Abstract*—Location is a basic property of an object. In the last decades, much attention has been paid to the precise localization and performance evaluation in Wireless Sensor Networks (WSN) areas. Ultra-wideband (UWB) and Inertial Measurement Unit (IMU) based localization method have been drawing attentions due to their advantageous performance. However, UWB suffers from the multipath effect and IMU suffers from error accumulation problem, which has limited their application prospects. Thus, the fusion of these two methods becomes necessary. Besides, in existing literatures, when estimating the positioning accuracy, it is generally assumed that the position of the base station is error free, which is not so consistent with reality. Thus, for the purpose of achieving high precision positioning in realistic conditions, we modelled the base station position error, IMU method error, and UWB method error, respectively. Based on these models, we derived 3-D CRLB (Cramer-Rao lower bound) and PCRLB (posterior Cramer-Rao lower bound) to characterize the spatial and temporal localization performance of this IMU/UWB fusion positioning method. We also compared CRLB with three commonly used localization algorithms and used it as a theoretical use case for CRLB. The experimental results show that the effect of base station position error on the positioning result cannot be ignored. CRLB and PCRLB can be used as benchmarks based on UWB and IMU fusion positioning system, and as the reference lower limit of the performance improvement of the positioning algorithms.**

***Index Terms*—sensor network, ultra-wideband, inertial measurement units, Cramer-Rao lower bound, base station error**

I. Introduction

WIRELESS sensor network (WSN) is composed of a large number of stationary or moving sensors in a self-organizing and multi-hop manner to cooperatively perceive, collect, process and transmit information of perceived objects in a network coverage area through wireless communication. It can be applied in many fields, such as military [1], emergency [2], industrial [3] and etc., to monitor various data information, and many of these monitoring information need to be associated with corresponding location information, so the acquisition of node location information in the sensor network is very important [4].

Global Positioning System (GPS) is an all-around, all-weather, full-time, high-precision satellite navigation system that provides global users with low-cost, high-precision navigation information such as 3-D position and speed [5]. However, in harsh environment, the effectiveness of GPS is limited in harsh environment such as dense building areas, where GPS signals cannot penetrate most of the obstacles [6]. New positioning technology is therefore needed to meet the demand for precise positioning in these harsh environment. Ultra-wideband (UWB) positioning can provide accurate distance measurement in harsh environment because of its accurate delay resolution and robustness, and is widely used in wireless sensor network positioning system [6-7]. However, UWB ranging method is susceptible to multipath effects and the relative geometric positional relationship between nodes [6]. In recent years, inertial navigation system (INS) as an auxiliary positioning method can compensate UWB's multipath effects and geometric topology problems. Inertial measurement units (IMU) such as accelerometers, gyroscopes, magnetometers, etc., can provide a series of continuous inertial information to improve positioning accuracy [8-9].

In regional positioning systems, the network usually consists of two types of nodes: anchor nodes (i.e., base stations) and target nodes [6]. It is generally assumed that the base station position is known and there is no error. The location of target node is unknown. Each node is equipped with a RF transceiver, and we can get the wireless signal characteristic parameters related to distance or angle when the target node performs radio communication with the base station. The commonly used wireless signal characteristic parameters include: time-of-arrival (TOA) [10-11], time-difference-of-arrival (TDOA) [12-13], arrival signal angle (Angle-of-arrival, AOA) [14-15] and received signal strength (RSS) [16-17]. Among them, the reliability of the correspondence between RSS and transmission distance is poor. AOA measurement relies on complex smart antenna arrays, and the technical feasibility is poor. TDOA requires high-precision synchronization technology support, while TOA can achieve ranging without synchronization. Therefore, TOA-based UWB ranging method is

Manuscript received 11 Mar. 2018. This work was supported by the National Key R&D Program of China (2016YFC0901303), the National Natural Science Foundation of China (NSFC) project (61671056, 61302065, 61304257, 61402033), the Beijing Natural Science Foundation project (4152036), and the Tianjin Special Program for Science and Technology (16ZXCXSF00150).

The authors are from School of Computer and Communication Engineering, University of Science and Technology Beijing, China.

widely used in WSN positioning system.

The location of the target node is uncertain because of the influence of random phenomena such as noise, fading, multipath, and non-line-of-sight propagation, which ultimately affects the positioning accuracy. Cramer-Rao lower bound (CRLB) defines the theoretical lower bound of the unbiased estimator variance and is used as a general criterion for evaluating the performance of a positioning system [18-20]. However, CRLB only focuses on the influence of the relationship between relative positions in spatial state on the accuracy of the positioning target, neglects the time information, and cannot meet the requirements of the time evaluation in the positioning system. The posterior Cramer-Rao lower bound (PCRLB) considers the time domain information [21-22] and can be used as another criterion for the performance evaluation of the positioning system.

The main contributions of this article are as follows:

- A IMU/UWB fusion based localization algorithm for WSN is presented, which can compensate the UWB multipath effect and IMU error accumulation problem;
- Base station positioning error is considered along with the performance evaluation process. In existing literatures, when assessing positioning accuracy, it is usually assumed that the base station position is completely accurate and error-free, but under normal circumstances, the base station position is obtained by GPS technology or other autonomous positioning technology [23]. These techniques also produce many errors due to signal interference and other factors, which results in the uncertainty of the base station location. Therefore, it is also very important to analyze the influence of the base station error on the positioning accuracy;
- Comprehensively, both spatial and temporal performance are evaluated in 3-D scenarios, with considering various factors in WSN. The existing research generally focuses on the CRLB and PCRLB in the 2-D case, rarely considering the CRLB and PCRLB in the 3-D case, especially when based on UWB and IMU fusion positioning method;
- We compare CRLB with three kinds of positioning algorithms: Least Squares positioning, Centroid positioning and Taylor expansion positioning. It further shows that CRLB can be used as a reference standard for the improvement of positioning algorithm.

The remainder of the paper is organized as follows. Section II introduces the fusion positioning method. Section III models the error from three perspectives including IMU method error, base station error, and UWB method error. Section IV deduces the CRLB and PCRLB under the above factors and performs the corresponding experimental verification. Section V compares CRLB with three kinds of localization algorithms and conclusions are drawn in section VI.

II. Fusion Positioning Method

A. IMU-based positioning method

IMU generally includes three single-axis accelerometers and three single-axis gyroscopes. Accelerometers detect the accelerations of the target in the carrier coordinate system. Gyroscopes detect the angular velocities of the target relative to the navigation coordinate system. By measuring the accelerations and angular velocities of the target in 3-D space, the step length and direction information are obtained through attitude calculation [24]. According to the step size and direction information, the target position of the next state can be predicted, which will not be described in detail here.

B. TOA-based UWB positioning method

TOA is a method of estimating the distance length by measuring the transmission time of wireless signals. The

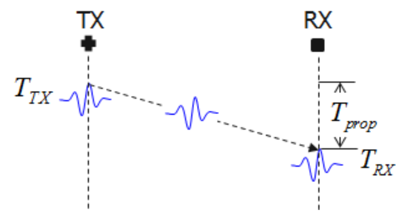

Fig. 1. The principle of TOA ranging

TOA ranging principle is shown in Figure 1.

In Fig.1, T_{TX} is the time when the target node sends the pulse signals, T_{RX} is the time when the base station receives the pulse signals, T_{prop} is the propagation time of the pulse signals in the medium. The propagation speed of the wireless signals in the air is equal to the speed of light, so the distance between the target node and the base station is given as

$$d_{TX-RX} = T_{prop} \times C = (T_{RX} - T_{TX}) \times C \tag{1}$$

where C indicates the speed of light, i.e., $C = 3 \times 10^8 \mathrm{m}/s$.

According to the distance of each state, we can use the relevant positioning algorithm to get the final position of the target node. At present, the most commonly used algorithms in the TOA positioning system include Least Square (LS) [25], Taylor Series expansion (TS) [26] and Centroid Localization [27], etc., which are not described in detail here.

C. Fusion Positioning method

The Kalman filter algorithm is an estimation method that estimates the state sequence of a dynamic system optimally, and makes the estimated value of the system state have a minimum mean square error [28]. It includes two parts: prediction and update. This paper uses the Kalman filter algorithm to achieve the integration of IMU and UWB multi-source data.

Let $\boldsymbol{m}_k = [x_k, y_k, z_k]^{\mathrm{T}}$, $k = 1, 2, \ldots, K$ denote the state vector of the mobile node in state *k*, where (x_k, y_k, z_k) denotes the 3-D coordinate of the node in world coordinate space and *K* denotes the total state observation number. Let $\boldsymbol{z}_k$ denote the measurement vector of the mobile node in state *k*, then the equation of state and observation equation for the system can be defined as

$$\begin{cases} \boldsymbol{m}_k = \boldsymbol{A}_k \boldsymbol{m}_{k-1} + \boldsymbol{q}_k, \\ \boldsymbol{z}_k = \boldsymbol{H}_k \boldsymbol{m}_k + \boldsymbol{r}_k, \end{cases} \tag{2}$$

where $\boldsymbol{q}_k$ indicates the process error, which is based on the error of the IMU, obeys a Gaussian distribution with a mean of 0 and a covariance of $\boldsymbol{Q}$. $\boldsymbol{r}_k$ denotes the measurement error, that is, the UWB ranging error, a Gaussian distribution with a mean of 0 and a covariance of $\boldsymbol{R}$. Matrix $\boldsymbol{A}_k$ and matrix $\boldsymbol{H}_k$ represent state transition matrix and measurement relation matrix, respectively.

We can use the Kalman filter algorithm to predict the position of the mobile node based on the state equation, and then update the position of the mobile node according to the measurement equation. Let $\bar{\hat{\boldsymbol{m}}}_k$ be a priori estimate of $\boldsymbol{m}_k$, i.e., the predicted value, and let $\hat{\boldsymbol{m}}_k$ denote an unbiased estimate, i.e., an updated value. The prior estimate of the error covariance is

ALGORITHM I KALMAN FILTER ALGORITHM

1. **Initialize** $\boldsymbol{m}_1$;
2. **Initialize** $\hat{\boldsymbol{m}}_1 = \hat{\boldsymbol{z}}_1, \boldsymbol{P}_1 = E[(\boldsymbol{m}_1 - \hat{\boldsymbol{m}}_1)(\boldsymbol{m}_1 - \hat{\boldsymbol{m}}_1)^{\mathrm{T}}]$;
3. **for** $k = 1, 2, \dots, K$,**do**
4. Predict the state, $\bar{\hat{\boldsymbol{m}}}_k = \boldsymbol{A}_k \hat{\boldsymbol{m}}_{k-1}$,
5. Predict state error covariance, $\bar{\boldsymbol{P}}_k = \boldsymbol{A}_k \boldsymbol{P}_{k-1} \boldsymbol{A}_k^{\mathrm{T}} + \boldsymbol{Q}$,
6. Compute Kalman gain, $\boldsymbol{G}_k = \bar{\boldsymbol{P}}_k \boldsymbol{H}_k^{\mathrm{T}} (\boldsymbol{H}_k \bar{\boldsymbol{P}}_k \boldsymbol{H}_k^{\mathrm{T}} + \boldsymbol{R})^{-1}$,
7. Update the state, $\hat{\boldsymbol{m}}_k = \bar{\hat{\boldsymbol{m}}}_k + \boldsymbol{G}_k (\boldsymbol{z}_k - \boldsymbol{H}_k \bar{\hat{\boldsymbol{m}}}_k)$,
8. Update state error covariance, $\boldsymbol{P}_k = (\mathbf{I} - \boldsymbol{G}_k \boldsymbol{H}_k) \bar{\boldsymbol{P}}_k$.
9. **end for**

$\bar{\boldsymbol{P}}_k = \boldsymbol{E}[(\boldsymbol{m}_k - \bar{\hat{\boldsymbol{m}}}_k)(\boldsymbol{m}_k - \bar{\hat{\boldsymbol{m}}}_k)^{\mathrm{T}}]$ and the posterior estimate is $\boldsymbol{P}_k = \boldsymbol{E}[(\boldsymbol{m}_k - \hat{\boldsymbol{m}}_k)(\boldsymbol{m}_k - \hat{\boldsymbol{m}}_k)^{\mathrm{T}}]$. Kalman filter algorithm is described in Algorithm 1.

III. ERROR MODELING

The fusion positioning method based on UWB and IMU will also produce some errors in the positioning process. Since the inertial information used in the attitude calculation process in the IMU-based positioning method has errors, the obtained step length information and direction information also have errors. UWB-based ranging positioning method knows the location of the base station in advance, but in general, the location of the base station is obtained by GPS technology which is also affected by factors such as noise, resulting in uncertainty in the location of the base station itself, thereby further affecting the positioning accuracy. In addition, when measuring the distance between the target node and the base station, the ranging error may also be caused due to environmental interference and other factors.

According to the above, we can conclude that the sources of error based on UWB and IMU fusion positioning methods are: 1) IMU step error and direction error, 2) base station error and 3) UWB ranging error.

Assume that the coordinates of the target node at the time k are $\boldsymbol{m}_k = [x_k, y_k, z_k]^{\mathrm{T}}$, and the coordinate of the nth base sta-

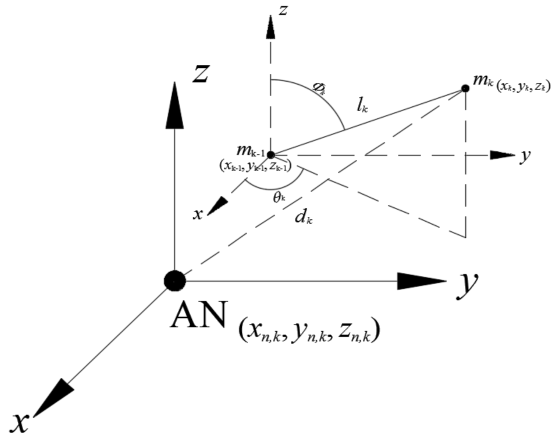

Fig. 2 The state transition of the target node

tion is $\boldsymbol{a}_n = [x_{n,k}, y_{n,k}, z_{n,k}]^{\mathrm{T}}, n = 1, 2, \dots, N$, where N is the number of anchor nodes. The schematic diagram of the state of the target node is shown in Fig.2.

The state information matrix of the target node is $\boldsymbol{m} = [\boldsymbol{m}_1, \boldsymbol{m}_2, \dots, \boldsymbol{m}_K]^{\mathrm{T}}$ and K is the total state number. For each element in the state information matrix, the following formula can be obtained by

$$\boldsymbol{m}_k = \boldsymbol{m}_{k-1} + l_k \boldsymbol{w}_k + \boldsymbol{r}_k, \tag{3}$$

where l_k is the moving step of the node from state k–1 to state k, $\boldsymbol{w}_k = [\sin\phi_k \cos\theta_k, \sin\phi_k \sin\theta_k, \cos\phi_k]^{\mathrm{T}}$ is the moving direction of the node, $\boldsymbol{r}_k$ the overall error caused by step error and direction error.

A. Error modeling based on IMU method

The step size estimate based on the IMU can be expressed as

$$\hat{l}_k = l_k + u_k, u_k \sim N(0, \sigma_{1,k}^2), \tag{4}$$

where l_k is the actual step size, i.e.,

$$l_k = \sqrt{(x_k - x_{k-1})^2 + (y_k - y_{k-1})^2 + (z_k - z_{k-1})^2}, \tag{5}$$

u_k is the step error and obeys the Gaussian distribution with a mean of 0 and a covariance of $\sigma_{1,k}^2$.

The vertical angle estimate based on the IMU can be expressed as

$$\hat{\phi}_k = \phi_k + v_k, v_k \sim N(0, \sigma_{2,k}^2), \tag{6}$$

where ϕ_k is the actual vertical angle, i.e.,

$$\phi_k = \arccos \frac{z_k - z_{k-1}}{l_k}, \tag{7}$$

v_k is the vertical angle error and obeys the Gaussian distribution with a mean of 0 and a covariance of $\sigma_{2,k}^2$.

The horizontal angle estimate based on the IMU can be expressed as

$$\hat{\theta}_k = \theta_k + \varepsilon_k, \varepsilon_k \sim N(0, \sigma_{3,k}^2), \tag{8}$$

where θ_k is the actual horizontal angle, i.e.,

$$\theta_k = \arctan \frac{y_k - y_{k-1}}{x_k - x_{k-1}}, \tag{9}$$

ε_k is the horizontal angle error and obeys the Gaussian distribution with a mean of 0 and a covariance of $\sigma_{3,k}^2$.

B. Base station error modeling

In the first section of this chapter, we define the coordinate of the nth base station as $\boldsymbol{a}_n = [x_{n,k}, y_{n,k}, z_{n,k}]^{\mathrm{T}}$, $n = 1, 2, ..., N$. Assuming that the base station coordinate errors are $\delta_{x_n}, \delta_{y_n}, \delta_{z_n}$, respectively, the actual estimation of the base station coordinate is

$$\begin{aligned} \hat{\boldsymbol{a}}_n &= [\hat{x}_{n,k}, \hat{y}_{n,k}, \hat{z}_{n,k}]^{\mathrm{T}} \\ &= [x_{n,k} - \delta_{x_n}, y_{n,k} - \delta_{y_n}, z_{n,k} - \delta_{z_n}]^{\mathrm{T}}, \end{aligned} \tag{10}$$

where $\delta_{x_n}, \delta_{y_n}, \delta_{z_n}$ obey Gaussian distributions with a mean of 0 and a variance of $\sigma_{\delta_{x_n}}^2, \sigma_{\delta_{y_n}}^2$, and $\sigma_{\delta_{z_n}}^2$, respectively.

C. Error modeling based on UWB method

The distance between the target node and the anchor node measured by the UWB ranging method is estimated as

$$\begin{aligned} \hat{d}_{n,k} &= \| \boldsymbol{m}_k - \hat{\boldsymbol{a}}_n \|_2 + e_{1,k} \\ &= d_{n,k} + e_{2,k} + e_{1,k} = d_{n,k} + e_k, \end{aligned} \tag{11}$$

where $d_{n,k}$ is the actual distance between the target node TN and the nth anchor node AN, i.e.,

$$d_{n,k} = \sqrt{(x_k - x_{n,k})^2 + (y_k - y_{n,k})^2 + (z_k - z_{n,k})^2}, \tag{12}$$

$e_{1,k}$ is the ranging error caused by the UWB method and obeys a Gaussian distribution with a mean of 0 and a variance of $\sigma_{4,k}^2$, i.e., $e_{1,k} \sim N(0, \sigma_{4,k}^2)$. $e_{2,k}$ is the ranging error caused by the base station error. Bring equation (10) into equation (11), and ignore the second-order error term, we can get

$$e_{2,k} \approx \frac{((x - x_{n,k})\delta_{x_n} + (y - y_{n,k})\delta_{y_n} + (z - z_{n,k})\delta_{z_n})}{d_{n,k}}, \tag{13}$$

so $e_{2,k} \sim N(0, \frac{((x - x_{n,k})^2 \sigma_{\delta_{x_n}}^2 + (y - y_{n,k})^2 \sigma_{\delta_{y_n}}^2 + (z - z_{n,k})^2 \sigma_{\delta_{z_n}}^2)}{d_{n,k}^2})$. Define $\sigma_{5,k}^2 = \frac{((x - x_{n,k})^2 \sigma_{\delta_{x_n}}^2 + (y - y_{n,k})^2 \sigma_{\delta_{y_n}}^2 + (z - z_{n,k})^2 \sigma_{\delta_{z_n}}^2)}{d_{n,k}^2}$, then $e_{2,k} \sim N(0, \sigma_{5,k}^2)$. Therefore, $e_k \sim N(0, \sigma_{4,k}^2 + \sigma_{5,k}^2)$. Define $\sigma_{6,k}^2 = \sigma_{4,k}^2 + \sigma_{5,k}^2$, then $e_k \sim N(0, \sigma_{6,k}^2)$.

IV. Positioning Performance Evaluation

In this section, we mainly introduce CRLB and PCRLB. We define $\nabla_a = [\frac{\partial}{\partial_{a_1}}, \frac{\partial}{\partial_{a_2}}, ..., \frac{\partial}{\partial_{a_M}}]^{\mathrm{T}}$ as a gradient vector, define $\boldsymbol{\Delta}_b^a = \boldsymbol{\nabla}_b \boldsymbol{\nabla}_a^{\mathrm{T}}$, define $p(a)$ as the probability density function of the random variable a, and define $\mathrm{tr}\{\bullet\}$ as the trace of the matrix.

A. Spatial Performance Evaluation

1) Derivation of CRLB

CRLB is represented as a theoretical lower limit for any unbiased estimation and is widely used to assess localization performance. Thus, we comprehensively derive the CRLB for 3D localization of IMU/UWB fusion method in WSNs to evaluate its spatial performance. Here comes some definitions.

If $\hat{\boldsymbol{m}}_k$ is an unbiased estimate of $\boldsymbol{m}_k$, then

$$\boldsymbol{E}\{(\hat{\boldsymbol{m}}_k - \boldsymbol{m}_k)^2\} \geq CRLB = \mathrm{tr}\{\boldsymbol{J}(\boldsymbol{m}_k)^{-1}\}, \tag{14}$$

where $\boldsymbol{J}(\boldsymbol{m}_k)$ is the Fisher information matrix [29].

Before solving the Fischer information matrix, we need to first define the joint probability density function as

$$\begin{aligned} &p(\hat{d}_k, \hat{l}_k, \hat{\phi}_k, \hat{\theta}_k, \hat{\boldsymbol{m}}_k) \\ &= \left\{ \prod_{n=1}^{N} p(\hat{d}_{n,k} \mid \boldsymbol{m}_k) \right\} \bullet p(\hat{l}_k \mid \boldsymbol{m}_{k-1}, \boldsymbol{m}_k) \\ &\bullet p(\hat{\phi}_k \mid \boldsymbol{m}_{k-1}, \boldsymbol{m}_k) \bullet p(\hat{\theta}_k \mid \boldsymbol{m}_{k-1}, \boldsymbol{m}_k), \end{aligned} \tag{15}$$

where $p(\hat{l}_k \mid \boldsymbol{m}_{k-1}, \boldsymbol{m}_k)$, $p(\hat{\phi}_k \mid \boldsymbol{m}_{k-1}, \boldsymbol{m}_k)$, $p(\hat{\theta}_k \mid \boldsymbol{m}_{k-1}, \boldsymbol{m}_k)$ and $p(\hat{d}_{n,k} \mid \boldsymbol{m}_k)$ can be obtained according to equations (4) ~ (13).

According to the joint probability density function, we can define the Fischer information matrix as

$$\boldsymbol{J}(\boldsymbol{m}_k)_{i,j} = -\boldsymbol{E}\left[\frac{\partial^2 \ln p(\hat{d}_k, \hat{l}_k, \hat{\phi}_k, \hat{\theta}_k, \hat{\boldsymbol{m}}_k)}{\partial m_{k,i} \partial m_{k,j}}\right], i, j = 1, 2, 3. \tag{16}$$

Bringing Equation (15) into Equation (16) can calculate each element of the Fischer Information Matrix, and further obtain CRLB.

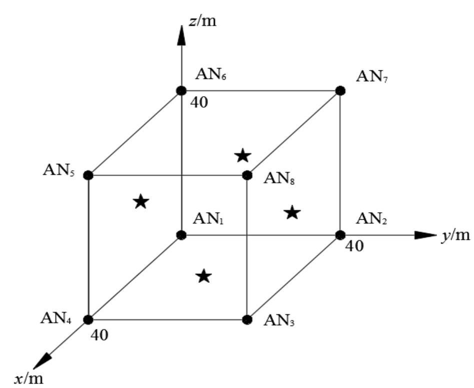

Fig. 3 The deployment of nodes in sensor network

2) Experimental verification

A 3-D stereoscopic sensor network environment is designed as shown in Fig. 3.

Eight anchor nodes ANs are deployed in the scene and distributed in eight corners. Target nodes TNs are distributed in the middle of the area. The dots in Fig. 3 represent the anchor nodes and the pentagrams represent the target nodes. Assume that the communication range of the anchor nodes can cover the entire area, and the anchor nodes can receive the required information from the target nodes.

CRLB reflects the influence of the relationship between relative positions in space on the accuracy of the positioning target. Assume that the target node performs a uniform linear motion along the x direction. The movement speed is 1m/s and the sampling interval is 1s. Then, $x_k - x_{k\text{-}1} = 1\text{m}$, $y_k - y_{k\text{-}1} = 0\text{m}$, $z_k - z_{k\text{-}1} = 0\text{m}$, and $l_k = \sqrt{(x_k - x_{k\text{-}1})^2 + (y_k - y_{k\text{-}1})^2 + (z_k - z_{k\text{-}1})^2} = 1\text{m}$.

We mainly analyze the impact of different situations on CRLB from the following two perspectives. Other comparative results can be found in [30].

1) Impact on CRLB when considering base station error and not considering base station error

Fig. 4.a and Fig. 4.b show the impact on the CRLB when considering the base station error and not considering the base station error in the case of 3-D, respectively. $\sigma_{\delta_{x_n}} = 0.2\text{m}$, $\sigma_{\delta_{y_n}} = 0.2\text{m}$, $\sigma_{\delta_{z_n}} = 0.2\text{m}$, $\sigma_{4,k} = 0.5\text{m}$. Since the base station error is only considered in the UWB ranging positioning, the CRLB based on a single UWB ranging method can reflect the impact of the base station error. From Fig. 4.a and Fig. 4.b, we can see that when considering the base station error, the positioning accuracy of the system will be reduced by at most 6 cm. This also means that it is necessary to accurately estimate the position of the base station before performing UWB positioning.

2) Impact on CRLB based on UWB and IMU fusion positioning method and single UWB ranging method

Fig. 5 shows the impact of the fusion positioning method on CRLB in 3-D scenes. The effects of base station errors on the results are not considered here. Assume that $\sigma_{1,k} = 0.5\text{m}$, $\sigma_{2,k} = 10^\circ$, $\sigma_{3,k} = 10^\circ$, and $\sigma_{4,k} = 0.5\text{m}$. Comparing Fig.5 with Fig. 4.b using a single UWB method, it can be seen that when the fusion positioning method is adopted, the positioning accuracy of the system can reach 0.108m at most. Comparing the results of Fig. 5 with the results of Fig. 4.b, the systematic error is significantly reduced and can be reduced by at most 0.263m.

B. Temporal performance Evaluation

1) Derivation of PCRLB

Sequential tracking problem is supposed to be a temporal problem other than a sole spatial one. These continuous information could be used to evaluate the performance of given algorithms. Thus, we extend the above CRLB to PCRLB with considering posterior information.

Before the derivation, we redefine the joint probability density function as

$$\begin{aligned} &p(\hat{d},\hat{l},\hat{\phi},\hat{\theta},\hat{\boldsymbol{m}}) \\ &= p(\hat{d}_0|\boldsymbol{m}_0)\prod_{k=1}^{K} p(\hat{l}_k \mid \boldsymbol{m}_{k-1},\boldsymbol{m}_k)\, p(\hat{\phi}_k \mid \boldsymbol{m}_{k-1},\boldsymbol{m}_k) \\ &p(\hat{\theta}_k \mid \boldsymbol{m}_{k-1},\boldsymbol{m}_k)\, p(\hat{d}_k \mid \boldsymbol{m}_k). \end{aligned} \tag{17}$$

To calculate the Fischer information matrix at state k, we define

$$p_k = p(\hat{\boldsymbol{d}}_{0:k},\hat{\boldsymbol{l}}_{0:k},\hat{\boldsymbol{\phi}}_{0:k},\hat{\boldsymbol{\theta}}_{0:k},\hat{\boldsymbol{m}}_{0:k}), \tag{18}$$

where $\hat{\boldsymbol{d}}_{0:k}$, $\hat{\boldsymbol{l}}_{0:k}$, $\hat{\boldsymbol{\phi}}_{0:k}$, $\hat{\theta}_{0:k}$, $\hat{\boldsymbol{m}}_{0:k}$ represent ranging, step length, vertical angle, horizontal angle and target coordinate vector from the start state to state k respectively.

Therefore,

$$\begin{aligned} &\boldsymbol{J}(\boldsymbol{m}_{0:k}) \\ &= \begin{bmatrix} \boldsymbol{E}\{-\Delta_{\boldsymbol{m}_{0:k-1}}^{\boldsymbol{m}_{0:k-1}} ln p_k\} & \boldsymbol{E}\{-\Delta_{\boldsymbol{m}_{0:k-1}}^{\boldsymbol{m}_k} ln p_k\} \\ \boldsymbol{E}\{-\Delta_{\boldsymbol{m}_k}^{\boldsymbol{m}_{0:k-1}} ln p_k\} & \boldsymbol{E}\{-\Delta_{\boldsymbol{m}_k}^{\boldsymbol{m}_k} ln p_k\} \end{bmatrix} \\ &= \begin{bmatrix} \boldsymbol{A}_k & \boldsymbol{B}_k \\ \boldsymbol{B}_k^{\mathrm{T}} & \boldsymbol{C}_k \end{bmatrix}. \end{aligned} \tag{19}$$

According to [31], the sub-matrix $\boldsymbol{J}_k$ can be obtained by pseudo-inverse of the matrix $\boldsymbol{J}(\boldsymbol{m}_{0:k})$, i.e.,

$$\boldsymbol{J}_k = \boldsymbol{C}_k - \boldsymbol{B}_k^{\mathrm{T}} \boldsymbol{A}_k^{-1} \boldsymbol{B}_k. \tag{20}$$

According to equations (17) and (18), the joint probability density for the k+1 state is

$$\begin{aligned} &p_{k+1} \\ &= p_k\, p(\hat{l}_{k+1} \mid \boldsymbol{m}_k,\boldsymbol{m}_{k+1})\, p(\hat{\phi}_{k+1} \mid \boldsymbol{m}_k,\boldsymbol{m}_{k+1})\, p(\hat{\theta}_{k+1} \mid \boldsymbol{m}_k,\boldsymbol{m}_{k+1}) \\ &p(\hat{d}_{k+1} \mid \boldsymbol{m}_{k+1}). \end{aligned} \tag{21}$$

According to the joint probability density of state k+1, we can find that

$$\boldsymbol{J}(\boldsymbol{m}_{0:k+1}) = \begin{bmatrix} \boldsymbol{A}_k & \boldsymbol{B}_k & \boldsymbol{0} \\ \boldsymbol{B}_k^{\mathrm{T}} & \boldsymbol{C}_k + \boldsymbol{H}_k^{11} & \boldsymbol{H}_k^{12} \\ \boldsymbol{0} & \boldsymbol{H}_k^{12} & \boldsymbol{\beta}_{k+1} + \boldsymbol{H}_k^{22} \end{bmatrix}, \tag{22}$$

where $\boldsymbol{H}_k^{11}$, $\boldsymbol{H}_k^{12}$, $\boldsymbol{H}_k^{22}$ reflect the posterior information from state k to state k+1, and $\boldsymbol{\beta}_{k+1}$ reflects the location information based on UWB ranging [30].

From $\boldsymbol{J}(\boldsymbol{m}_{0:k+1})$ and $\boldsymbol{J}_k$ we can get the Fischer information matrix for state k+1, i.e.,

$$\begin{aligned} &\boldsymbol{J}_{k+1} \\ &= \boldsymbol{\beta}_{k+1} + \boldsymbol{H}_k^{22} - \begin{bmatrix} \boldsymbol{0} & \boldsymbol{H}_k^{12} \end{bmatrix} \begin{bmatrix} \boldsymbol{A}_k & \boldsymbol{B}_k \\ \boldsymbol{B}_k^{\mathrm{T}} & \boldsymbol{C}_k + \boldsymbol{H}_k^{11} \end{bmatrix} \begin{bmatrix} \boldsymbol{0} \\ \boldsymbol{H}_k^{12} \end{bmatrix} \\ &= \boldsymbol{\beta}_{k+1} + \boldsymbol{H}_k^{22} - \boldsymbol{H}_k^{12} (\boldsymbol{J}_k + \boldsymbol{H}_k^{11})^{-1} \boldsymbol{H}_k^{12}. \end{aligned} \tag{23}$$

Due to the step error and the directional error obey Gaussian distribution, $\boldsymbol{H}_k^{11} = \boldsymbol{H}_k^{12} = \boldsymbol{H}_k^{22} = \boldsymbol{H}_k$ can be calculated. The solution of $\boldsymbol{H}_k$ can be referenced [22, 30].

In summary, the posterior Fisher information matrix is

$$\boldsymbol{J}_{k+1} = \boldsymbol{\beta}_{k+1} + \boldsymbol{H}_k - \boldsymbol{H}_k (\boldsymbol{J}_k + \boldsymbol{H}_k)^{-1} \boldsymbol{H}_k. \tag{24}$$

According to the SMW (Sherman–Morrison–Woodbury) formula [32], it can be further simplified as

$$\boldsymbol{J}_{k+1} = \boldsymbol{\beta}_{k+1} + (\boldsymbol{H}_k^{-1} + \boldsymbol{J}_k^{-1})^{-1}, \tag{25}$$

where $\boldsymbol{\beta}_{k+1}$ reflects the information based on UWB, $\boldsymbol{H}_k$ reflects information based on IMU.

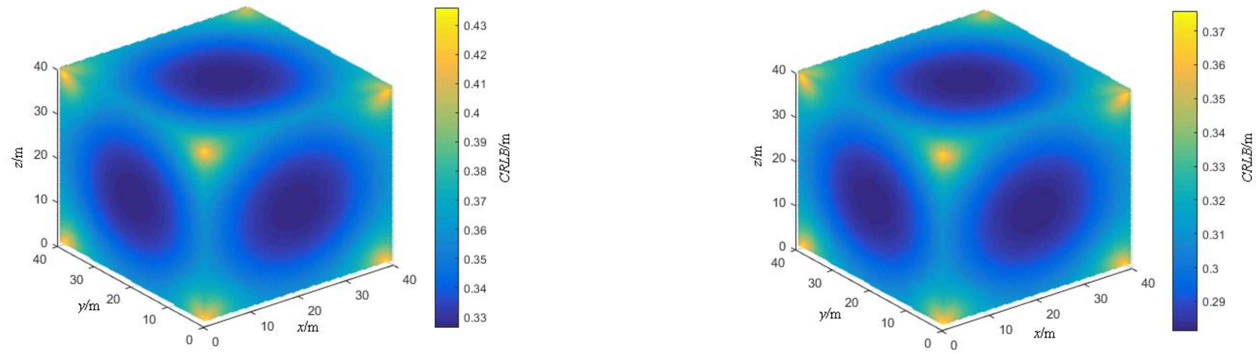

a) CRLB when considering anchor position error   b) CRLB without considering anchor position error

Fig. 4 CRLB when considering base station error and not considering base station error

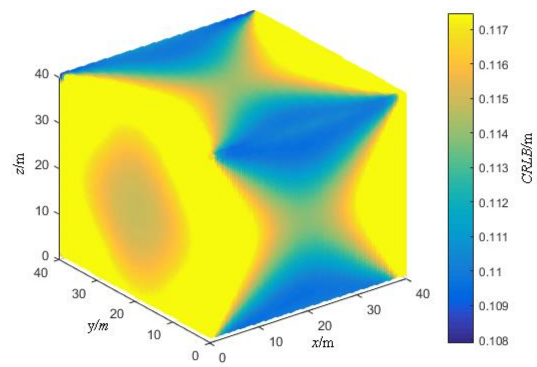

Fig. 5 CRLB based on the proposed hybrid method

2) Experimental verification

We use the root mean square of PCRLB to evaluate the performance of the fusion positioning method. The root mean square of the PCRLB can be represented by $\frac{1}{L}\sum_{i=1}^{L} P_k^i$, where P_k^i represents the PCRLB of the mobile node in state k in the ith Monte Carlo experiment, and L represents the total number of Monte Carlo experiments. In this paper, L is taken as 1000. Assume that the initial position of the mobile node is (1, 1, 1), and the mobile node performs random motion in the scene to ensure the equilibrium of the entire target node's movement process. Since UWB compensates for the cumulative error of the IMU during the entire motion, it is assumed that the step error and the directional error remain the same throughout the entire motion. The step error measured by the IMU is proportional to the actual step size, i.e., $\sigma_{1,k} = \eta l_k$, where η is the proportional coefficient. Assume that $\sigma_{2,k} = 10^\circ$, $\sigma_{3,k} = 10^\circ$, $\sigma_{4,k} = 0.5\text{m}$, $\sigma_{\delta_{x_n}} = 0.2\text{m}$, $\sigma_{\delta_{y_n}} = 0.2\text{m}$, $\sigma_{\delta_{z_n}} = 0.2\text{m}$. Random motion is generated by randomly generating 3 directions of velocity, and the sampling interval is 1 s.

We mainly analyze the influence of different situations on PCRLB from the following two perspectives. Other comparison results can be found in reference [30].

1) Impact on PCRLB when considering base station error and not considering base station error

FIg.6 shows the PCRLB in the fusion location method when considering the error of the base station and not considering the

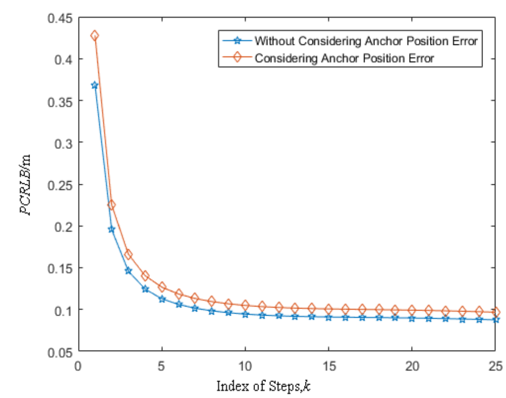

Fig. 6 Effect of anchor position error on PCRLB

error of the base station. It can be seen from Fig. 6that the error of the base station will have a certain impact on the positioning accuracy of the system and the accuracy will be reduced by at least 4cm.

2) Impact on PCRLB based on different positioning Methods

Fig. 7 shows the theoretical minimum error that can be achieved using the UWB based method alone (i.e., no IMU

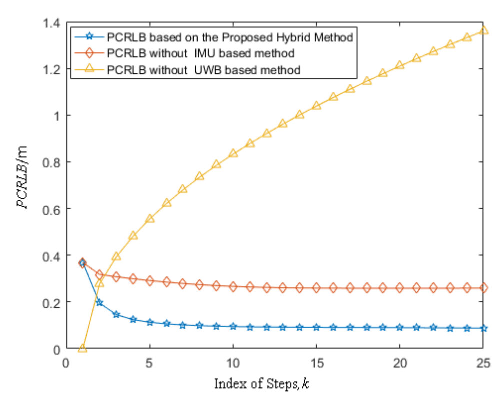

Fig. 7 PCRLB of different positioning methods

method), the IMU based method alone (i.e., no UWB ranging method), and the fusion positioning method under a 3-D environment.

It can be seen from Fig. 7 that: ① Compared with the single UWB based method, the fusion positioning method significantly improves the positioning accuracy of the mobile node. ② Compared with a single IMU based method, the fusion positioning method compensates for the cumulative error problem based on the IMU method and tends to be stable after a certain time.

V. Typical application of Evaluation methods

The Cramer-Rao Lower Bound (CRLB) characterizes the lower limit of the position error that a positioning system can achieve in a timed and empty condition the positioning system can achieve under certain time and space conditions. It can be used to evaluate and design the positioning method and base station deployment in certain scenarios. It can also be used to evaluate and verify the performance of different algorithms [2]. Based on the above theoretical derivation, using CRLB as an example, we compare the theoretical performance of different algorithms in the IMU/UWB fusion system.

We mainly verify the three most commonly used positioning algorithms, namely, centroid positioning, least squares positioning, and Taylor series expansion positioning. Two simulation scenarios are considered, with considering base station error and not considering base station error.

The result of the positioning algorithm is represented by the root mean square error of RMSE, i.e.,

TABLE I
Comparison of RMSE for Different Location Algorithms and CRLB

	Not considering base station error	Considering base station error
Centroid	0.6814	0.7725
Least-Square	0.6465	0.6639
Taylor Series Expansion	0.4850	0.5230
CRLB	0.1128	0.1213

$$RMSE = \sqrt{\frac{\sum_{i=1}^{n} \varepsilon_i^2}{n}}, \tag{26}$$

where ε_i denotes the positioning error at each sample point and n denotes the number of samples. The comparison results are shown in Table 1.

From Table 1, we can see that when the scenes are the same, the positioning results of the three positioning algorithms are all different. Compared with least-square positioning and centroid positioning, the Taylor series expansion positioning method has better positioning performance in both cases. However, there is still much room for improvement when compared with CRLB.

Scenes Algorithm RMSE

VI. Conclusions

This paper proposes a fusion positioning method based on UWB and IMU in wireless sensor networks. This method can improve the positioning accuracy while compensating UWB multipath effects and IMU error accumulation problems. In order to evaluate the positioning accuracy under real-world conditions, base station position error, IMU method error and UWB method error are modeled. Based on these models, CRLB and PCRLB in 3-D environment are deduced. Finally, the paper compares CRLB with three commonly used localization algorithms. Experimental results show that the effect of base station position error on positioning results cannot be ignored. CRLB and PCRLB can be used as benchmarks based on UWB and IMU fusion positioning systems and as reference lower limits for performance improvement of location algorithms.

References

[1] J. Rantakokko, P. Strömbäck and et al. Accurate and reliable soldier and first responder indoor positioning: Multi-sensor systems and cooperative localization[J]. IEEE Wireless Communication, 2011, 18(2): 10-18

[2] S. Gandhi, A. Ganz and G. Mullett. FIREGUIDE: Firefighter Guide and Tracker[C]. IEEE Engineering in Medicine and Biology Society (EMBC'10), Buenos Aires, Argentina, 2010

[3] Jaehyun Park and Jangmyung Lee. A Beacon Color Code Scheduling for the Localization of Multiple Robots[J]. IEEE Trans. Industrial Informatics, 2011, 7(3): 467-475

[4] Yu P. A review: wireless sensor networks localization [J]. Journal of Electronic Measurement & Instrument, 2011, 25(5):389-399

[5] Zhang J B, Zhang P Z, Kun-Kun D U. Wireless sensor networks time synchronization based on GPS[J]. Transducer & Microsystem Technologies, 2009, 28(6):31-33

[6] Yuan S, Win M Z. Fundamental Limits of Wideband Localization— Part I: A General Framework [J]. IEEE Transactions on Information Theory, 2010, 56(10):4956-4980

[7] Fontana R J. Recent system applications of short-pulse ultra-wideband (UWB) technology [J]. Microwave Theory & Techniques IEEE Transactions on, 2004, 52(9):2087-2104

[8] Lee S, Kim B, Kim H, et al. Inertial sensor-based indoor pedestrian localization with minimum 802.15.4a configuration[J]. IEEE Trans on Industrial Informatics, 2011, 7(3):455-466

[9] Xu Cheng, He Jie, Zhang Xiaotong, et al. Geometrical kinematic modeling on human motion using method of multi-sensor fusion [J]. Information Fusion, 2017,41:243-254

[10] Xu Cheng, He Jie, Zhang Xiaotong, et al. Toward near-ground localization: Modeling and applications for TOA ranging error [J]. IEEE Trans on Antennas & Propagation, 2017, 65(10):5658-5662

[11] Dardari D, Chong C C, Win M Z. Improved lower bounds on time-of-arrival estimation error in realistic UWB channels[C] //Proc of the 6th IEEE Int Conf on Ultra-wideband. Piscataway, NJ: IEEE, 2006:531-537

[12] Li Cong, Zhuang Weihua. Non-line-of-sight error mitigation in TDOA mobile location[C] //Proc of the 20th Global Telecommunications Conf. Piscataway, NJ: IEEE, 2001:680-684

[13] Ho K C, Chan Y T. Solution and performance analysis of geolocation by TDOA [J]. IEEE Trans on Aerospace & Electronic Systems, 1993, 29(4):1311-1322

[14] Xu Jun, Ma Maode, Law C L. AOA cooperative position localization[C] //Proc of the 27th Global Telecommunications Conf. Piscataway, NJ: IEEE, 2008:1-5

[15] Venkatraman S, Caffery J J. Hybrid TOA/AOA techniques for mobile location in non-line-of-sight environments[C] //Proc of the IEEE Wireless Communications & Networking Conf. Piscataway, NJ: IEEE, 2004:274-278

[16] Zhong Chen, Eliasson J, Makitaavola H. A cluster-based localization method using RSSI for heterogeneous wireless sensor networks[C] //Proc of the 6th Int Conf on Wireless Communications Networking and Mobile Computing. Piscataway, NJ: IEEE, 2010:1-6

[17] Patwari N, Hero A O. Using proximity and quantized RSS for sensor localization in wireless networks[C] //Proc of the 2nd ACM Int Conf on Wireless Sensor networks & applications. New York: ACM, 2003:20-29
[18] Tseng P H, Feng Kaiten. Derivation of CRLB for liner least square estimator in wireless location systems [J]. Wireless Networks, 2012, 18(7):735-747
[19] Shaban H A, Abou E M, Buehrer R M. Toward a highly accurate ambulatory system for clinical gait analysis via UWB radios [J]. IEEE Trans on Information Technology in Biomedicine, 2010, 14(2):284-291
[20] Zhang Yueyue, Zhu Yaping, Shen Liangfeng. A semidefinite relaxation approach to positioning in hybrid sensor networks[C] //Proc of the 85th IEEE Vehicular Technology Conf. Piscataway, NJ: IEEE, 2016:1-5
[21] He Ziming, Ma Yi, Tafazolli R. Posterior Cramer-Rao bound for inertial sensors enhanced mobile positioning under the random walk motion model [J]. IEEE Wireless Communications Letters, 2012,1(6):629-632
[22] Geng Yishuang, Pahlavan K. Design, implementation, and fundamental limits of image and RF based wireless capsule endoscopy hybrid localization [J]. IEEE Trans on Mobile Computing, 2016, 15(8):1951-1964
[23] Yu K. 3-d localization error analysis in wireless networks [J]. Wireless Communications IEEE Transactions on, 2007, 6(10):3472-3481
[24] Zhang R H, Jia H G, Tao C, et al. Attitude solution for strapdown inertial navigation system based on quaternion algorithm [J]. Optics & Precision Engineering, 2008
[25] Zhang B F, Liu T P, Han Y, et al. 3-Dimension location algorithm research based on TOA[J]. Computer Engineering & Design, 2007
[26] Ren B, Hui-Bin X U. A Taylor Series Expansion TOA Based on Total Least Square in UWB[J]. Science Technology & Engineering, 2013
[27] Chen H, Huang P, Martins M, et al. Novel Centroid Localization Algorithm for Three-Dimensional Wireless Sensor Networks[C]// International Conference on Wireless Communications, NETWORKING and Mobile Computing. IEEE, 2010:1-4
[28] Benini A, Mancini A, Marinelli A, et al. A Biased Extended Kalman Filter for Indoor Localization of a Mobile Agent using Low-Cost IMU and UWB Wireless Sensor Network[J]. IFAC Proceedings Volumes, 2012, 45(22):735-740
[29] Balan R. The fisher information matrix and the CRLB in a non-AWGN model for the phase retrieval problem[C]// International Conference on Sampling Theory and Applications. IEEE, 2015:178-182
[30] Duan Shihong, Yao Cui, Xu Cheng, et al. Towards wireless sensor network: Performance evaluation of UWB and IMU fusion positioning[J]. Journal of Computer Research and Development, 2018,55
[31] Tichavsky P, Muravchik C H, Nehorai A. Posterior Cramer-Rao bounds for discrete-time nonlinear filtering[J]. Signal Processing IEEE Transactions on, 1998, 46(5):1386-1396
[32] Deng C Y. A generalization of the Sherman–Morrison–Woodbury formula[J]. Applied Mathematics Letters, 2011, 24(9):1561-1564